Structural reliability analysis of a laminated plate using the Reissner-Mindlin model and the finite element method

Lucas M. de Macedo[1], Paulo T. R. Mendonça[2], Wellison J. S. Gomes[1]

[1]*Department of Civil Engineering, Center for Optimization and Reliability in Engineering (CORE), Federal University of Santa Catarina*
R. João Pio Duarte Silva, 205, Florianópolis, 88037-000, Santa Catarina, Brazil
lmacedo.ufba@gmail.com, wellison.gomes@ufsc.br
[2] *Department of Mechanical Engineering, Federal University of Santa Catarina*
Technology Center, Florianópolis, 88040-900, Santa Catarina, Brazil
paulo.tarso@ufsc.br

Abstract. The use of anisotropic laminated plates as structural elements has become increasingly common due to their ability to emphasize desired mechanical characteristics and reduce undesired ones, depending on the laminate stacking sequence and angles. Although applications of structural optimization methods to define the optimum laminate stacking angle are common in the literature, analyses of the influence of this angle on the behavior of the plate are relevant when seeking to increase laminate efficiency. In addition, consideration of the uncertainties that affect the structural response of these elements is still under development and open to discussion. Structural reliability is a suitable tool for dealing with these uncertainties. This article aims to analyze the influence of the stacking angle on the first-ply failure probability, taking into account the probability distributions of the random variables involved. The First Order Reliability method and Tsai-Wu failure criteria are employed. The plate considered herein is subjected to transversal static loading and made up of orthotropic laminae in oblique directions. The structure is modelled using the Finite Element Method, with Reissner-Mindlin kinematic theory in the linear elastic regime. The results indicated significant variability in the failure probability depending on the stacking angle.

Keywords: structural reliability, laminated plate, finite element method, probabilistic first-ply failure load.

1 Introduction

In the field of civil engineering, composite materials have become increasingly common, due to the search for materials that ensure more sustainable development compared to cement and steel, characterized by their high environmental impact in manufacturing, and also to their ability to enhance specific material properties, as noted by Wasim *et al.* [1]. This application is particularly prevalent in structural engineering, where composites contribute to improved mechanical strength, resistance to high temperatures, and impact protection for infrastructure and vehicles. An example of the application of laminated composites in civil engineering, according to Chróścielewski *et al.* [2], is the use of carbon fibers or glass fibers reinforced with plastic in the construction of walkway structures.

In general, laminated composites are subject to complex stress states, and various uncertainties affect their behavior, so that structural reliability analysis may be necessary. The literature contains numerous studies that vary in the type of structural analysis (linear or non-linear), the type of loading (transverse or in-plane), the geometry of structural elements (such as plates with holes), the application of different failure criteria, and different definitions of failure criteria. Kam *et al.* [3] investigated the effect of ply stacking sequence on the reliability of

plates subjected to static loading in the non-linear regime with large deflections, using the maximum stress rupture criterion to determine an optimal orientation in plate design. In a related study, Kam *et al.* [4] analyzed plate reliability based on the concept of the first ply failure, exploring how different probability distributions of random variables influence the probability of plate failure. Additionally, Sriramula [5] provided an overview of stochastic modeling approaches for fiber-reinforced plastic composites from a probabilistic standpoint, aiming to classify the uncertainties inherent in such modeling.

In this context, the objective of this paper is to assess the impact of the stacking angle of a symmetrical laminated composite plate on its probability of failure.

2 Formulations for the structural reliability analysis of laminated plates

2.1 Composite laminated plate

As a linear elastic regime is assumed for the material's response, the deformations are obtained using Hooke's law, as presented by Mendonça [6], and are written for a ply k

$$\boldsymbol{\sigma} = \bar{\mathbf{Q}}^{\mathrm{k}}\boldsymbol{\varepsilon} \quad \text{and} \quad \boldsymbol{\tau}_{\mathbf{s}} = \bar{\mathbf{C}}^{\mathrm{k}}\boldsymbol{\gamma}_{\mathbf{c}}, \tag{1}$$

$$\boldsymbol{\sigma} = \left\{\boldsymbol{\sigma}_{\mathbf{x}}, \boldsymbol{\sigma}_{\mathbf{y}}, \boldsymbol{\tau}_{\mathbf{xy}}\right\}^{T} \quad \text{and} \quad \boldsymbol{\tau}_{\mathbf{s}} = \left\{\boldsymbol{\tau}_{\mathbf{yz}}, \boldsymbol{\tau}_{\mathbf{xz}}\right\}^{T}, \tag{2}$$

$$\boldsymbol{\varepsilon} = \left\{\boldsymbol{\varepsilon}_{\mathbf{x}}, \boldsymbol{\varepsilon}_{\mathbf{y}}, \boldsymbol{\gamma}_{\mathbf{xy}}\right\}^{T} \quad \text{and} \quad \boldsymbol{\gamma}_{\mathbf{c}} = \left\{\boldsymbol{\gamma}_{\mathbf{yz}}, \boldsymbol{\gamma}_{\mathbf{xz}}\right\}^{T}, \tag{3}$$

where $\bar{\mathbf{Q}}$ and $\bar{\mathbf{C}}$ are the reduced stiffness matrices for in-plane and shear stresses, respectively. These matrices depend on the properties in the main directions of the ply, namely the moduli of elasticity in the longitudinal and transverse directions (E_1 and E_2), the shear modulus in the three planes (G_{12}, G_{13} and G_{23}), the Poisson's ratio also in the three planes (ν_{12}, ν_{13} and ν_{23}).

The plies used in laminates are generally reinforced by unidirectional fibers aligned in direction 1, making them symmetrical about this same axis. Direction 1 is defined as the longitudinal direction, direction 2 as the transverse direction, and direction 3 as the normal direction. Considering that the thickness of the ply is much greater than the diameter of the fibers, this material is termed transversely isotropic in the 2-3 plane, and the relationships shown in eq. (4) are demonstrated in Mendonça [6]

$$E_3 = E_2, \quad \nu_{13} = \nu_{12}, \quad \nu_{23} = \nu_{32}, \quad G_{13} = G_{12}, \quad G_{23} = \frac{E_2}{2(1+\nu_{23})} \quad \text{and} \quad S_{13} = S_{12}. \tag{4}$$

The first-order kinematic model is defined by the following hypotheses

$$\begin{aligned} u(x,y,z) &= u^0(x,y,t) + z\psi_x(x,y), \\ v(x,y,z) &= v^0(x,y,t) + z\psi_y(x,y), \\ w(x,y,z) &= w(x,y), \end{aligned} \tag{5}$$

where u^0, v^0, w, ψ_x, and ψ_y are the generalized displacement functions with respect to the reference surface.

Linear strain-displacement relationships are defined by

$$\varepsilon_x = \frac{\partial u}{\partial x}, \quad \varepsilon_y = \frac{\partial v}{\partial y}, \quad \varepsilon_z = 0, \quad \gamma_{xy} = \frac{\partial u}{\partial y} + \frac{\partial v}{\partial x}, \quad \gamma_{yz} = \frac{\partial w}{\partial y} + \psi_y \quad \text{and} \quad \gamma_{xz} = \frac{\partial w}{\partial x} + \psi_x. \tag{6}$$

It is possible to identify and name the constituent parts of deformations

$$\boldsymbol{\varepsilon} = \boldsymbol{\varepsilon}^{\mathbf{0}} + \mathrm{z}\boldsymbol{\kappa}, \tag{7}$$

where $\boldsymbol{\varepsilon}^{\mathbf{0}}$ represents the membrane deformations responsible for the in-plane deformations of the reference surface, indicating an extension or contraction and $\boldsymbol{\kappa}$ represents the curvatures.

The normal forces (**N**), shear forces (**V**), and bending moments (**M**) in a laminate are obtained by

$$\begin{Bmatrix} \mathbf{N} \\ \mathbf{M} \end{Bmatrix} = \mathbf{C}\begin{Bmatrix} \boldsymbol{\varepsilon}^{\mathbf{0}} \\ \boldsymbol{\kappa} \end{Bmatrix} \quad \text{and} \quad \mathbf{V} = \mathbf{E}\boldsymbol{\gamma}_{\mathbf{c}}, \tag{8}$$

$$\mathbf{C} = \begin{bmatrix} \mathbf{A} & \mathbf{B} \\ \mathbf{B} & \mathbf{D} \end{bmatrix}, \tag{9}$$

where A_{ij}, B_{ij} and D_{ij} with i,j = 1,2 and 6, and $E_{ij}$with i,j = 4 and 5

$$A_{ij} = \sum_{k=1}^{N} \bar{Q}_{ij}^{k}(z_k - z_{k-1}), \quad B_{ij} = \left(\frac{1}{2}\right)\sum_{k=1}^{N} \bar{Q}_{ij}^{k}(z_k^2 - z_{k-1}^2), \quad D_{ij} = \left(\frac{1}{3}\right)\sum_{k=1}^{N} \bar{Q}_{ij}^{k}(z_k^3 - z_{k-1}^3) \quad \text{and} \quad (10)$$

$$E_{ij} = k\sum_{k=1}^{N} \bar{C}_{ij}^{k}. \quad (11)$$

The equilibrium equations are defined by Zienkiewicz and Taylor [7]

$$\frac{\partial \sigma_x}{\partial x} + \frac{\partial \tau_{xy}}{\partial y} + \frac{\partial \tau_{xz}}{\partial z} + \rho b_x = 0 \quad \text{and} \quad \frac{\partial \tau_{xy}}{\partial x} + \frac{\partial \sigma_y}{\partial y} + \frac{\partial \tau_{yz}}{\partial z} + \rho b_y = 0. \quad (12)$$

2.2 Finite Element Method (FEM) and stress smoothing

The stiffness matrices **K** and the vector of consistent forces **F** are obtained by the Principle of Virtual Work for the first-order kinematic method (Mindlin). The in-plane stresses are obtained at a point *(x,y)* of an element *e* by

$$\boldsymbol{\sigma}^{\mathrm{xl_k}} = \bar{\mathbf{Q}}^{\mathrm{k}}\{\boldsymbol{\varepsilon}^0 + \mathrm{z}\boldsymbol{\kappa}\} \quad \text{and} \quad \begin{Bmatrix}\boldsymbol{\varepsilon}^0 \\ \boldsymbol{\kappa}\end{Bmatrix}^{\mathrm{e}} = \mathbf{B}^{\mathrm{e}}\mathbf{U}^{\mathrm{e}}, \quad (13)$$

where **B** represents the rows of the deformation matrix associated with $\boldsymbol{\varepsilon}^{\mathbf{0}}$ and $\boldsymbol{\kappa}$, and **U** is the vector of FEM nodal displacement values. The transverse stresses are obtained by integrating the equations in (11)

$$\tau_{xz}^{i}(z) = \tau_{xz}^{i}(-H/2) - \int_{-H/2}^{z}\left[\frac{\partial \sigma_x}{\partial x} + \frac{\partial \tau_{xy}}{\partial y}\right]dz \quad \text{and} \quad \tau_{yz}^{i}(z) = \tau_{yz}^{i}(-H/2) - \int_{-H/2}^{z}\left[\frac{\partial \tau_{xy}}{\partial x} + \frac{\partial \sigma_y}{\partial y}\right]dz. \quad (14)$$

The stress components in the ply's principal directions are obtained by

$$\boldsymbol{\sigma}^{\mathbf{1l_k}} = \mathbf{T}^{\mathrm{k}}\boldsymbol{\sigma}^{\mathrm{xl_k}} \quad \text{and} \quad \boldsymbol{\tau}^{\mathrm{1l_k}} = \mathbf{T}_{\mathbf{c}}^{\mathrm{k}}\boldsymbol{\tau}^{\mathrm{xl_k}}, \quad (15)$$

where $\mathbf{T}^{\mathbf{k}}$ and $\boldsymbol{T}_c^k$ denote the rotation matrices of the ply *k*, defined by

$$\mathbf{T}^{\mathrm{k}} = \begin{bmatrix} \cos^2\theta & \mathrm{sen}^2\theta & 2\mathrm{sen}\theta\cos\theta \\ \mathrm{sen}^2\theta & \cos^2\theta & -2\mathrm{sen}\theta\cos\theta \\ -\mathrm{sen}\theta\cos\theta & \mathrm{sen}\theta\cos\theta & \cos^2\theta - \mathrm{sen}^2\theta \end{bmatrix} \quad \text{and} \quad \mathbf{T}_{\mathbf{c}}^{\mathrm{k}} = \begin{bmatrix} \cos\theta & -\mathrm{sen}\theta \\ \mathrm{sen}\theta & \cos\theta \end{bmatrix}. \quad (16)$$

The stress smoothing and recovery procedure employed are based on the Zienkiewicz-Zhu method as presented in Zienkiewicz and Zhu [8]. This method assumes that the values of $\boldsymbol{\varepsilon}^{\mathbf{0}}$and $\boldsymbol{\kappa}$ are calculated at a set of sample points on the mesh, which are then used to generate a continuous smoothed approximation of degree p, consistent with the displacements, in the form

$$\boldsymbol{\varepsilon}^0(x) = \mathbf{N}^e(x)\mathbf{E} \quad \text{and} \quad \boldsymbol{\kappa}(x) = \mathbf{N}^k(x)\mathbf{K}, \quad (17)$$

where the matrices $\mathbf{N}^e(x)$ and $\mathbf{N}^k(x)$ are constructed using the same displacement interpolation functions employed in the FEM model. **E** and **K** represent the nodal values of membrane deformations and curvature obtained through the smoothing process. Consequently, the recovered in-plane stresses are

$$\boldsymbol{\sigma}(x,z) = \mathbf{Q}^{\mathrm{k}}\left[\mathbf{N}^{\mathrm{e}}(x)\mathbf{E} + z\mathbf{N}^{\mathrm{k}}(x)\mathbf{K}\right]. \quad (18)$$

2.3 Tsai-Wu criterion

The Tsai-Wu failure criterion, proposed in 1971, originates from the von Mises yield criterion for isotropic materials, adapted for use with orthotropic materials as discussed in Lopez *et al.* [9]. According to Mendonça [6], this criterion allows for the definition of the following limit state function:

$$g(\mathbf{X}) = 1 - \left(\left(\frac{1}{\mathrm{X_t}} - \frac{1}{\mathrm{X_c}}\right)\sigma_1 + \left(\frac{1}{\mathrm{Y_t}} - \frac{1}{\mathrm{Y_c}}\right)\sigma_2 + \frac{\sigma_{12}}{\mathrm{X_tX_c}} + \frac{\sigma_{22}}{\mathrm{Y_tY_c}} + \left(\frac{\tau_{12}}{\mathrm{S_{12}}}\right)^2 - \frac{\sigma_1\sigma_2}{\sqrt{\mathrm{X_tX_cY_tY_c}}}\right), \quad (19)$$

where $\mathbf{X}$ = {$\mathrm{X_t}$, $\mathrm{X_c}$, $\mathrm{Y_t}$, $\mathrm{Y_c}$, $\mathrm{S_{12}}$, σ_1, σ_2 and τ_{12}}.

2.4 Probabilistic first-ply failure load analysis

The probabilistic first-ply failure analysis involves assessing the stress state in each ply of the laminate and evaluating its failure probability based on a selected failure criterion. It assumes that failure occurs when the first ply reaches the criterion. According to the assumptions previously made, in-plane deformations vary linearly through the laminate thickness, while in-plane stresses vary linearly within each ply, and transverse stresses vary parabolically.

2.5 Structural Reliability and the First Order Reliability Method

Given a vector of random variables **X** describing uncertainties affecting the structural response, with its respective joint probability density function $f_{\boldsymbol{X}}(\mathbf{x})$, and considering a limit state function $g(\boldsymbol{X})$ associated with a specific failure mode where negative values indicate failure, the failure probability related to this failure mode, as outlined in Melchers *et al.* [10], is given by

$$P_f = P[G(\mathbf{X}) \leq 0] = \int \ldots \int_{g(\boldsymbol{X})\leq 0} f_{\boldsymbol{X}}(\mathbf{x}) d\mathbf{x}. \tag{20}$$

With a few exceptions, the integration of the above equation cannot be performed analytically. Therefore, it is possible to simplify the probability density function in the integrand using iterative techniques to obtain reliable estimates of failure probabilities.

The First Order Reliability Method (FORM), as described by Mínguez [11], aims to determine the failure probability given by eq. (19) through three steps:

1. transform the vector of random variables of the problem **X**, which follows a given joint probability distribution, into a vector of random variables Y with a standard normal distribution (zero mean and unit standard deviation);

2. identify the most probable point of failure in the standard normal space, known as the design point;

3. linearize the surface of the limit state equation at the design point and compute the result analytically.

The obtained result is typically approximate due to the common occurrence of non-normal distributions, correlated variables, and non-linear limit state equations. The search for the design point can be facilitated by using algorithms such as the improved Hassofer, Lind, Rackwitz and Fiessler (iHLRF) method.

3 Results and discussion

To evaluate the influence of the ply stacking angle on the failure probability of a symmetrical laminated composite plate under transverse loading, the plate is modeled using the FEM. It has a rectangular geometry with dimensions $a = 500\text{mm}$ and $b = 250\text{mm}$, and is simply supported. The mesh is composed of 4x4 quadrilateral Lagrangian elements with 9 nodes. The model adopts the first-order kinematic theory of Reissner-Mindlin within the linear-elastic regime. The stiffness matrices, **K**, and the force vector, **F**, are computed using Gauss-Legendre numerical integration, with selective subintegration of 2x2 points. Stresses are extracted and smoothed using a uniform grid of points distributed across the element. The Tsai-Wu failure criterion, commonly referenced in the literature, is employed. FORM is employed to estimate failure probabilities.

As shown in Figure 1, the laminate consists of 4 orthotropic plies arranged symmetrically with orientations of $[\theta, -\theta, -\theta, \theta]$. The thicknesses of the plies are $h_1 = h_4 = 25\text{mm}$ and $h_2 = h_3 = 1{,}5h_1 = 37{,}5\text{mm}$, determined using the ratio $a/H = 4$, where H represents the total thickness of the laminate.

In the proposed analysis, the quadratic approximation method is employed to find the root of the limit state function in the search for the load that leads to failure.

The plate is subjected to a distributed static load *q(x,y)*, given by

$$q(x,y) = q_0 sen\left(\frac{\pi x}{a}\right) sen\left(\frac{\pi y}{b}\right), \tag{21}$$

where q_0 represents the magnitude of the load.

Considering various stacking angles and values for the maximum loading intensity, the results shown in Figure 2 were obtained. It is assumed that each ply is composed of carbon fibers embedded in an epoxy matrix,

with mechanical properties and statistical characterizations as detailed in Table 1, following Kimiaeifar [12].

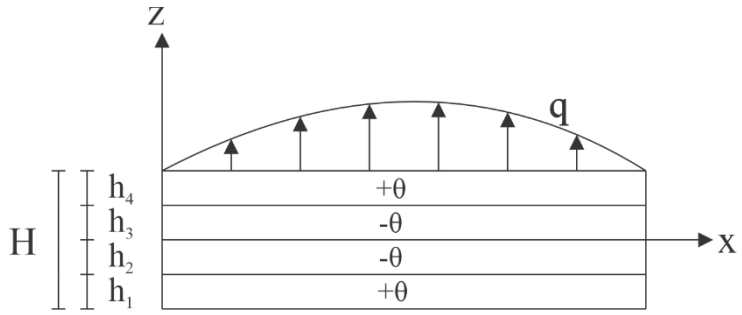

Figure 1: Cross-sectional view of the analyzed case.

Table 1. Statistical characterization of variables

Mechanical properties	Symbol	Distribution	Mean	COV
Longitudinal modulus of elasticity [MPa]	E_1	Lognormal	131000	0,106
Transverse modulus of elasticity [MPa]	$E_2 = E_3$	Lognormal	8000	0,136
Poisson's ratio	$v_{12} = v_{13} = v_{23}$	Lognormal	0,3	0,18
In-plane shear modulus 12[MPa]	$G_{12} = G_{13}$	Lognormal	5000	0,1
Shear modulus in plane 23 [MPa]	G_{23}	Lognormal	4000	0,1
Longitudinal tensile strength [MPa]	X_t	Normal	1150	0,135
Longitudinal compressive strength [MPa]	X_c	Normal	750	0,13
Transverse tensile strength [MPa]	Y_t	Weibull	47	0,104
Transverse compressive strength [MPa]	Y_c	Weibull	68	0,11
Shear strengths in planes 12, 13 and 23 [MPa]	$S_{12} = S_{13} = S_{23}$	Weibull	59	0,1

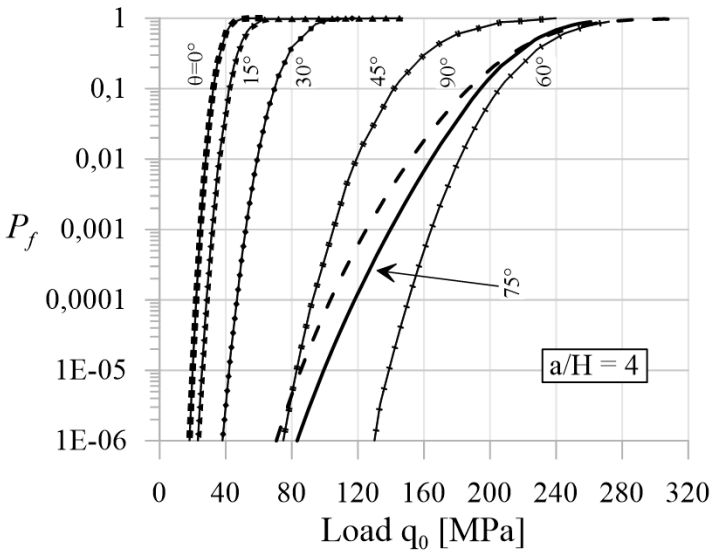

Figure 2: Probability of failure as a function of maximum loading intensity and stacking angle.

Analysis focusing on the load value is common in the design of composite elements. It is observed that within the 0° to 90° range, at a fixed failure probability, increasing the stacking angle allows for higher supported loads, with maximum values observed at the 60° angle among those analyzed. Conversely, lower load values are acceptable for angles such as 75° and 90°.

Setting a target loading value, such as 120 MPa, reveals that the laminate with the lowest failure probability is at the 60° stacking angle, with a failure probability lower than 10^{-6}. Note that at a 75° angle the failure probability associated with this loading level increases to about 10^{-4}.

Analyses can also be conducted based on target failure probabilities. For a 1-year return period, considering moderate consequences of failure and average costs for enhancing structural safety, the Joint Committee on Structural Safety (JCSS) [13] recommends a target failure probability of 10^{-5}. For this target value, it is observed, for instance, that the plate with a stacking angle of 45° could withstand loads of approximately 80 MPa, whereas for a 30° angle, the acceptable load reduces to about half of the former.

4 Conclusion

This study investigates the impact of the stacking angle of plies on the probability of failure, considering a simply supported rectangular plate under sinusoidal loading. The Tsai-Wu failure criterion is employed to define the plate's limit state function, assuming that the failure of any single ply results in the failure of the entire plate.

The results revealed significant variability in the probability of plate failure depending on the stacking angle. For instance, at a maximum loading intensity of 80 MPa, the probability of failure is approximately 100% for stacking angles of 0° and 15°, whereas it is less than 10^{-5} for angles of 45°, 60°, 75° and 90°. This highlights the importance of selecting an appropriate stacking angle to ensure acceptable levels of reliability for the structural element. Additionally, it was observed that among the analyzed angle values, the 60° angle consistently exhibited the highest levels of reliability across all considered loading intensities.

Ultimately, tools such as the one developed here can aid in the design of composite plates, proving applicable in both research and engineering practice.

Acknowledgements. This work is supported by the National Council for Technological and Scientific Development (CNPq) via grant 301756/2022-8.

Authorship statement. The authors hereby confirm that they are the sole liable persons responsible for the authorship of this work, and that all material that has been herein included as part of the present paper is either the property (and authorship) of the authors or has the permission of the owners to be included here.

References

[1] M. Wasim *et al.*. Future directions for the application of zero carbon concrete in civil engineering - A review. Case Studies in Construction Materials, [s. l.], v. 17, 2022.
[2] J. Chróścielewski *et al.*. A novel sandwich footbridge - Practical application of laminated composites in bridge design and in situ measurements of static response. Composites Part B: Engineering, [s. l.], v. 126, p. 153-161, 2017.
[3] T. Y. Kam, S. C. Lin, K. M. Hsiao. Reliability analysis of nonlinear laminated composite plate structures. Composite Structures, [s. l.], v. 25, p. 503-510, 1993.
[4] T. X. Kam, E. S. Chang. Reliability formulation for composite laminates subjected to first-ply failure. Composite Structures, [s. l.], v. 38, p. 441-452, 1997.
[5] S. Sriramula, M. K. Chryssanthopoulos. Quantification of uncertainty modeling in stochastic analysis of FRP composites. [S. l.: s. n.], 2009.
[6] P. T. de Mendonça. Composite Materials & Sandwich Structures. 2nd. ed. Florianópolis: Orsa Maggiore, 2019.
[7] O.C, Zienkiewicz; R.L, Taylor. The Finite Element Method Fifth edition Volume 1: The Basis. [S. l.: s. n.], 2000. v. 5
[8] O.C, Zienkiewicz, J. Z. Zhu. The superconvergent patch recovery and a posteriori error estimates. Part 1: The recovery technique. International Journal for Numerical Methods in Engineering, [s. l.], v. 33, n. 7, p. 1331-1364, 1992.
[9] R. H. Lopez, M. A. Luersen, E. S. Cursi. Optimization of laminated composites considering different failure criteria. Composites Part B: Engineering, [s. l.], v. 40, n. 8, p. 731-740, 2009.
[10] R. E. Melchers, A. T. Beck. Structural Reliability Analysis and Prediction. 3. ed. [S. l.: s. n.], 2018.
[11] R. Mínguez. Probability and Statistics for Engineers. [S. l.: s. n.], 2012.
[12] A. Kimiaeifar *et al.*. Asymptotic Sampling for reliability analysis of adhesive bonded stepped lap composite joints. Engineering Structures, [s. l.], v. 49, p. 655-663, 2013.
[13] JCSS Probabilistic Model Code. [S. l.: s. n.], 2001.